CDF/PUB/CDF/PUBLIC/9351
Draft 3.0
July 24, 2008

Using Drell-Yan to Probe the Underlying Event in Run 2 at CDF

Deepak Kar[1], Rick Field[2]

University of Florida, Gainesville, FL
On Behalf of the CDF Collaboration

Abstract

We study the event topology in Drell-Yan lepton-pair production in proton-antiproton collisions at 1.96 TeV in Run 2 at CDF. We use the direction of the lepton-pair on an event by event basis to define three regions of $\eta - \phi$ space; toward, away and transverse. The transverse and toward regions are very sensitive to the underlying event. The data are corrected back to the particle level and are then compared with the PYTHIA tune AW. The properties of the underlying event are examined as a function of the lepton-pair transverse momentum. The data are also compared with a previous analysis on the behavior of the underlying event in high transverse momentum jet production. The goal is to improve our understanding and modeling of the high energy collider events.

[1]dkar@phys.ufl.edu
[2]rfield@phys.ufl.edu

1 Introduction

The goal of this analysis is to present measurements sensitive to the underlying event that are corrected back to the particle level so that they can be used to tune the QCD Monte Carlo models without requiring CDF detector simulation and to compare with a similar analysis done with the Tevatron jet data.

1.1 Underlying Event in a Typical Collider Event

A typical 2-to-2 hard scattering event in a proton-antiproton collision at the hadron colliders as shown in the Fig. 1. The incoming fundamental particles are the quarks and gluons inside the hadrons and the strong force is the dominant interaction.

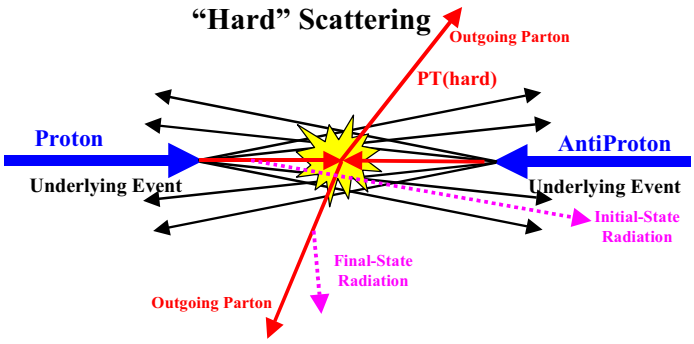

Figure 1: Components of a 2-2 Hard Scattering

Except the two hard scattered outgoing partons - the landscape is dominated by initial and final state radiation (caused by bremsstrahlung and gluon emission), resonance decays, multiple parton interaction (additional 2-to-2 scattering within the same event), hadronization, beam beam remnants (particles that come from the breakup of the proton and antiproton) and so on.

We define the 'underlying event' as everything except the two outgoing hard scattered

'jets' and consists of the 'beam-beam remnants' plus initial and final-state radiation[1]. However experimentally, it is impossible to seperate out the two components. The 'hard scattering' component consists of the outgoing two 'jets' plus initial and final-state radiation. The 'beam-beam remnants' are what is left over after a parton is knocked out of each of the initial two beam hadrons as in Fig. 3. It is the reason hadron-hadron collisions are more 'messy' than electron-positron annihilations and no one really knows how it should be modeled. Also, it is possible that multiple parton scattering, as in Fig. 2 contributes to the 'underlying event'. In addition to the hard 2-to-2 parton-parton scattering and the 'beam-beam remnants', sometimes there is a second 'semi-hard' 2-to-2 parton-parton scattering that contributes particles to the "underlying event" as in Fig. 2.

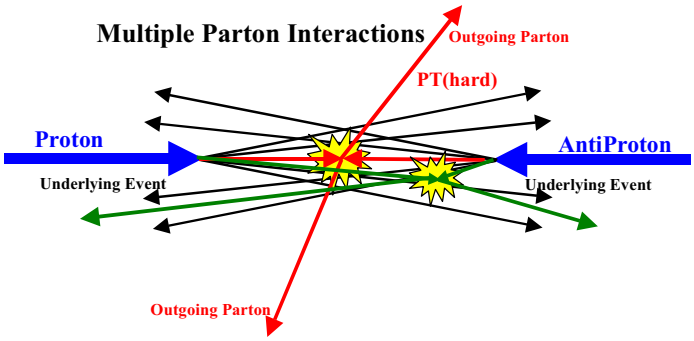

Figure 2: Multiple Parton Interactions

1.2 Transverse, Toward and Away Regions

We would now define and look at the different regions at a collider event. The angle $\Delta\phi = \phi - \phi_{leadingjet}$ is the relative azimuthal angle between charged particles and the direction of hard scattered leading jet. Later we would be looking at lepton pair production from Z boson, $\Delta\phi$ would then be determined relative to the direction of Z boson. Now we

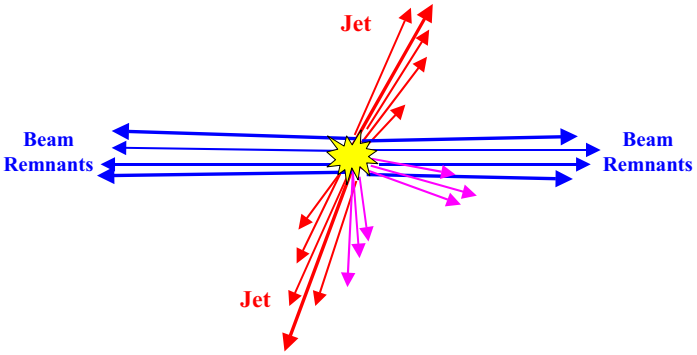

Figure 3: Beam Beam Remnants

can split the central region, defined between $|\eta| < 1$ as in Fig. 4.

- $|\Delta\phi| < 60^\circ$ as toward region.
- $60^\circ < |\Delta\phi| < 120^\circ$ as Transverse region. And,
- $|\Delta\phi| > 120^\circ$ as away region.

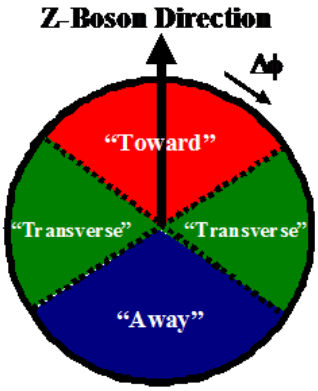

Figure 4: Different Regions in $\eta - \phi$ space

For hard scattered jets, where the relative azimuthal angle is with respect to the leading jet direction, the transverse regions are the most sensitive to underlying events, since they

are perpendicular to the plane of 2-to-2 hard scattering. For them we have outgoing jets in transverse regions, almost impossible to separate them out from the background.

As illustrated in next Figure, we define MAX and MIN transverse regions which help to separate the hard component (initial and final-state radiation) from the beam-beam remnant component. MAX (MIN) refer to the transverse region containing largest (smallest) number of charged particles or to the region containing the largest (smallest) scalar $p_T$sum of charged particles, on an event by event basis. One expects that the transMAX region will pick up the hardest initial or final-state radiation while both the transMAX and transMIN regions should receive beam-beam remnant contributions. Hence one expects the transMIN region to be more sensitive to the beam-beam remnant component of the underlying event, while the transMAX minus the transMIN (*i.e.*, transDIF) is very sensitive to hard initial and final-state radiation.

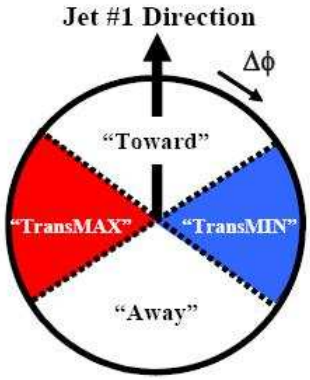

Figure 5: TransMAX and transMIN Regions.

1.3 The Drell Yan Process

Quarks and antiquarks from the incoming hadron beams annihilate to produce a virtual photon or Z^0, which decays to a lepton pair (e^+e^- or $\mu^+\mu^-$).

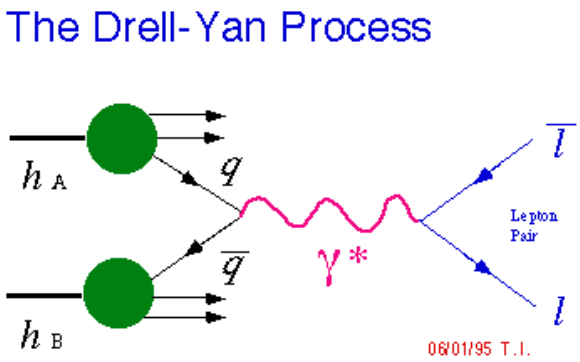

Figure 6: Drell Yan Process

Let us compare the underlying events in a hard scattering as in Fig. 1 with underlying events in Drell Yan process.

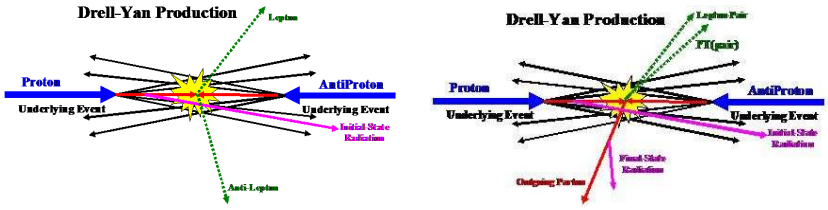

Figure 7: Underlying event in Drell-Yan. Left: Low P_T, Right: High P_T

By looking at the diagram we can see that essentially everything other than the final lepton-antilepton pair is the underlying event for the low P_T case. For Drell-Yan it is easy to identify and remove leptons (since they are the colorless components) from the transverse and toward regions to study the underlying event.

Single Z Bosons are produced with large P_T via the ordinary QCD sub processes, generating additional gluons via bremsstrahlung resulting in multi-parton final states fragmenting into hadrons and forming away-side jets. The transverse region is perpendicular to the hard scattering and once we remove the lepton pair from the toward region we are left with only underlying event in these two regions.

So we can see not only Drell Yan events are a clean probe of the underlying event but also we can study the underlying event as a function of lepton pair transverse momentum or invariant mass. Comparing them with high P_T jet production would help us to learn more about underlying event in general. And at the same time we would be able to look at Z boson P_T distribution, which would an extra way to constrain our underlying event model.

2 Analysis Strategy

2.1 Data Selection

We analyze the high P_T electron and muon Data and corresponding PYTHIA[2] tune AW[3] (tuned to fit the underlying event and the Z-boson P_T distribution measured in Run 1[4]) samples, as shown in Table 1. We analyzed data corresponding to the luminosity of approximately 2.7 fb^{-1}. We select only events having one and only one vertex within $|Z_{vtx}| < 60$ cm. It measures the distance of the $p\overline{p}$ collision event vertex from the center of the detector in z direction. To ensure that a track for each charged particle is well measured by the tracking system, we need this requirement.

Table 1: Data and Monte Carlo samples used in this analysis

Lepton	Monte Carlo	DATA
Electron	Drell- Yan Z/gamma* $\rightarrow ee$ sample	high-P_T Central electrons
Muon	Drell- Yan Z/gamma* $\rightarrow \mu\mu$ sample	high-P_T CMUP and CMX muons

2.2 Lepton Selection and Pair Formation

The electron and muon selections are based on the standard CDF high P_T electron and muon[5] selection criteria. An electron is a cluster of electromagnetic energy with with $E_T >$ 18 GeV and $|\eta| < 1.1$ matched to a trcak with $P_T > 10$ GeV/c with further requirements on position matching and shower shape in the CES. We look at central electrons, with tight and loose cuts described in [5]. We also remove conversions from photon by finding the partner track during the electron selection[6]. We look at the CMUP and CMX muons. A muon is a track with $P_T > 18$ GeV/c and $|\eta| < 1$ and a track segment in the muon chamber that matches the extrapolated position of the track. The only extra cut we make is on χ^2/DoF (the track χ^2 cut is based on the COT of the parent track and it is assumed that the number of degrees of the freedom is 5 less than the number of COT hits) - which helps to eliminate cosmic muons. Apart from that, to get rid of cosmic muons, we also use a Time of Flight (TOF) cosmic filter, as the time difference between the muons recorded in the upper and lower half of the detector is expected to be very small for muons not coming from cosmic rays.

The lepton pairs are formed by oppositely charged leptons, with the requirement that z_0 of the two leptons must pass $|z_0^1 - z_0^2| < 4$ cm, to ensure that both leptons came from the same primary collision. For electrons, we form pairs with at least one tight electron, as

defined earlier. For Muons, there is no such distinction.

We focus on the region of the lepton pair invariant mass between 70 and 110 GeV/c^2, which we refer to as the Z-region hereafter. Approximately 65,000 electron and muon pairs combined passed our selection criteria and are used in the analysis. We use the same selection critrea for data and detector level Monte Carlo.

The $Z \rightarrow e^+e^-$ and $Z \rightarrow \mu^+\mu^-$ data sample contains backgrounds mainly from QCD jets and W+jets. Studies[5] have shown that these backgrounds are negligible at the region of Z.

2.3 Charged Particle Selection

Only charged particles in the region of 0.5 GeV/c $< P_T <$ 150 GeV/c and $|\eta| < 1$, where efficiency is high are considered. The upper limit of P_{Tmax} cut is chosen as 150 GeV/c to prevent miss-measured tracks with very high P_T from contributing to the observables. The tracks are defined to be loose and tight according to track $|d_0|$ (transverse impact parameter defined as the minimum distance between the track and the primary vertex in the plane transverse to the beam direction - small value means the particle orginates from near the interaction region) and track $|\Delta z|$ (measured longitudinal distance between the mesaured track and the primary vertex). We also make sure none of the charged particles are electrons coming from pair production from photon[6].

2.4 Observables

Some of the observables that are studied in this analysis are described in Table 2. Since we would be studying regions in $\eta - \phi$ space with different areas, as defined in Section 1.2

we will construct densities by dividing by the area. The mean charged particle $< P_T >$ is constructed on an event by event basis and then averaged over the events. For the average P_T and P_{Tmax} we require that there is at least one charged particle present. The P_{Tsum} (hence the P_{Tsum} density) is taken to be zero if there are no charged particles present.

Table 2: Observables

Observable	Particle Level	Detector Level
Lepton P_T	P_T of the lepton pair	P_T of the lepton pair, formed by at least one tight lepton.
Lepton P_T Squared	P_T squared of the lepton pair	P_T squared of the lepton pair, formed by at least one tight lepton.
Charged Density	Number of charged particles per unit $\eta - \phi$	Number of 'good' charged tracks per unit $\eta - \phi$
$< P_T >$	Average P_T of charged particles	Average P_T of 'good' charged tracks
P_T Sum Density	Scalar P_T Sum of charged particles per unit $\eta - \phi$	Scalar P_T Sum of 'good' charged tracks per unit $\eta - \phi$
P_{TMax}	Maximum P_T of charged particle	Maximum P_T of 'good' charged tracks

2.5 Correcting Back to Particle Level

We use the ratio of the generator level Monte Carlo result and the detector level Monte Carlo result as our correction factor for correcting the data back to the particle level. Our generator level results are formed by adding both electron and muon results together, since in theory, they are expected to and indeed are found to be consistant. We put in the same kinematic cuts on both the particle level Monte Carlo and the detector level Monte carlo and data - we require that,

- Individual lepton $P_T > 20$ GeV/c,
- Individual lepton $|\eta| < 1$, and
- Lepton pair $|\eta| < 6$.

2.6 Systematic Uncertainties

We correct the data back to particle level in three different ways for electron, and in two different ways for muon. We take the differences at particle level between (1) loose-tight and tight-tight electron selection and (2) loose and tight track cuts for charged particles as sysmatic uncertainties for electron data. For muon data, the differences between loose and tight track cuts are taken as systematic uncertainties. We add the different systematic errors in quadrature, and add the statistical error with that in quadrature with that to draw one combined error bar. We observed that the differences between different cuts do not produce a significant systematic uncertainty and the dominant contribution to our total uncertainties are statistical. When comparing with the dijet 'underlying event' data later, we would see that they have much smaller statistical (hence overall) uncertainties, as dijet events have more statistics.

3 Results

3.1 Z Region Results

As mentioned earlier, we present results on the underlying event observables in the events with the lepton pair invarinat mass in the z boson region, *i.e* 70-110 GeV/c^2. The presented results refer to all the charged particles with $P_T > 0.5$ GeV/c and $|\eta| < 1$. We have combined

our electron and muon results. The underlying event observables defined in Section 2.4 are shown as a function of the lepton pair p_T in Figs. 7-26. We present results for lepton pair $P_T < 100$ GeV/c, above which we do not have enough statistics. The underlying event observables are found to be reasonably flat with the increasing lepton pair P_T in the transverse and toward regions, but goes up in the away region to balance lepton pairs. We overlay transverse and toward regions for each observable in the same plot for comparison purpose, and then overlay the away region with them to see this effect.

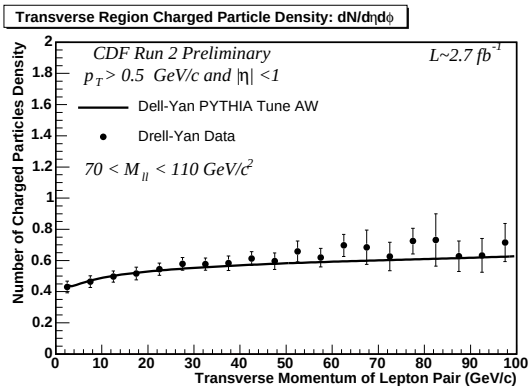

Figure 8: Transverse Region Charged Multiplicity Density, Data Corrected, Electron and Muon Data Combined ($P_T > 0.5$ GeV/c and $|\eta| < 1$). Solid line represents PYTHIA Tune AW predictions and the data are corrected back to particle level (with errors that include both the statistical error and the systematic uncertainty).

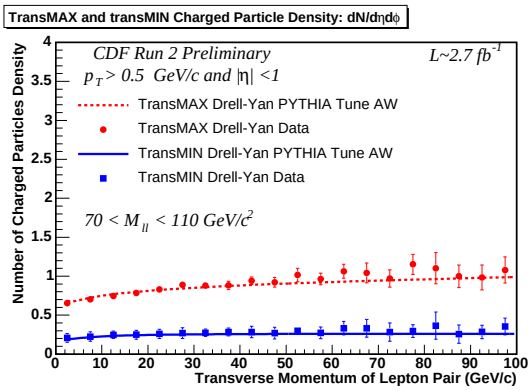

Figure 9: TransMAX and MIN Region Charged Multiplicity Density, Data Corrected, Electron and Muon Data Combined ($P_T > 0.5$ GeV/c and $|\eta| < 1$). Lines represent PYTHIA Tune AW predictions and the data are corrected back to particle level (with errors that include both the statistical error and the systematic uncertainty).

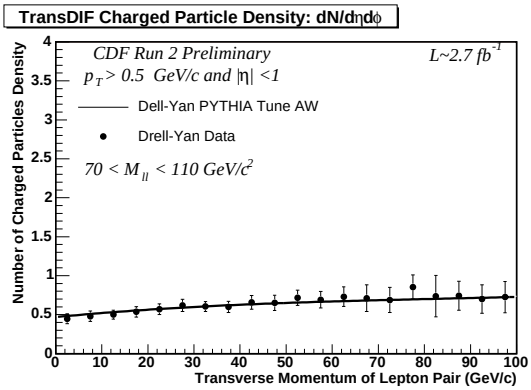

Figure 10: TransDIF Region Charged Multiplicity Density, Data Corrected, Electron and Muon Data Combined ($P_T > 0.5$ GeV/c and $|\eta| < 1$). Solid line represents PYTHIA Tune AW predictions and the data are corrected back to particle level (with errors that include both the statistical error and the systematic uncertainty).

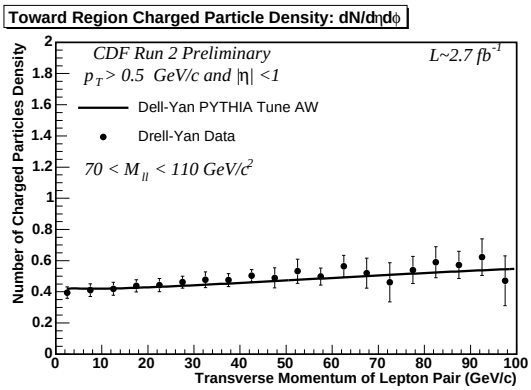

Figure 11: Toward Region Charged Multiplicity Density, Data Corrected, Electron and Muon Data Combined ($P_T > 0.5$ GeV/c and $|\eta| < 1$). Solid line represents PYTHIA Tune AW predictions and the data are corrected back to particle level (with errors that include both the statistical error and the systematic uncertainty).

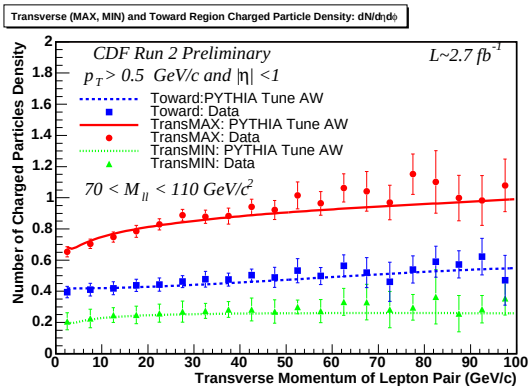

Figure 12: Transverse and Toward Region Charged Multiplicity Density, Data Corrected, Electron and Muon Data Combined ($P_T > 0.5$ GeV/c and $|\eta| < 1$). Lines represent PYTHIA Tune AW predictions and the data are corrected back to particle level (with errors that include both the statistical error and the systematic uncertainty).

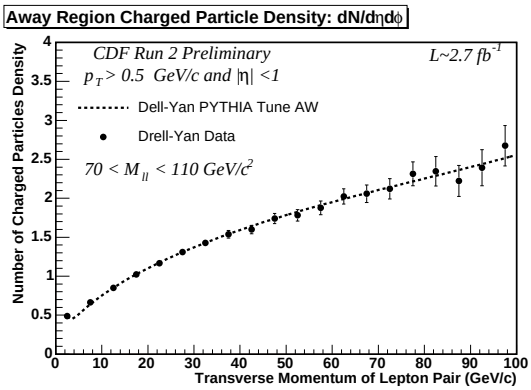

Figure 13: Away Region Charged Multiplicity Density, Data Corrected, Electron and Muon Data Combined ($P_T > 0.5$ GeV/c and $|\eta| < 1$). Solid line represents PYTHIA Tune AW predictions and the data are corrected back to particle level (with errors that include both the statistical error and the systematic uncertainty).

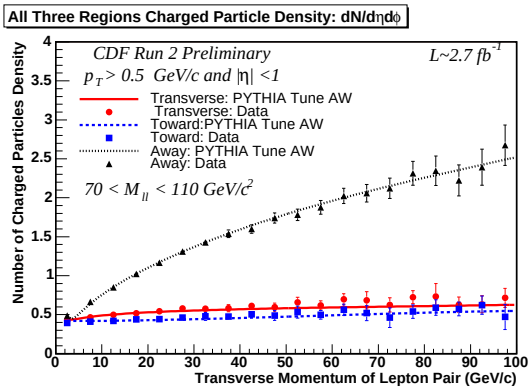

Figure 14: All Three Regions Charged Multiplicity Density, Data Corrected, Electron and Muon Data Combined ($P_T > 0.5$ GeV/c and $|\eta| < 1$). Lines represent PYTHIA Tune AW predictions and the data are corrected back to particle level (with errors that include both the statistical error and the systematic uncertainty).

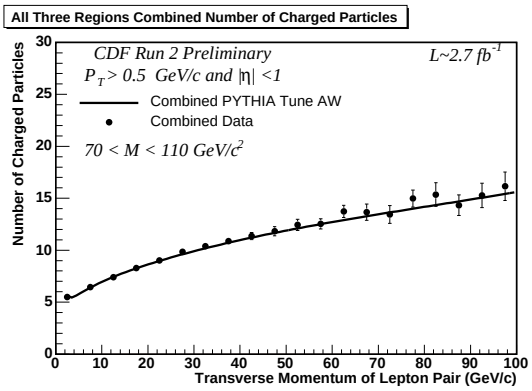

Figure 15: All Three Regions Charged Multiplicity Density Added, Data Corrected, Electron and Muon Data Combined ($P_T > 0.5$ GeV/c and $|\eta| < 1$). Solid line represents PYTHIA Tune AW predictions and the data are corrected back to particle level (with errors that include both the statistical error and the systematic uncertainty).

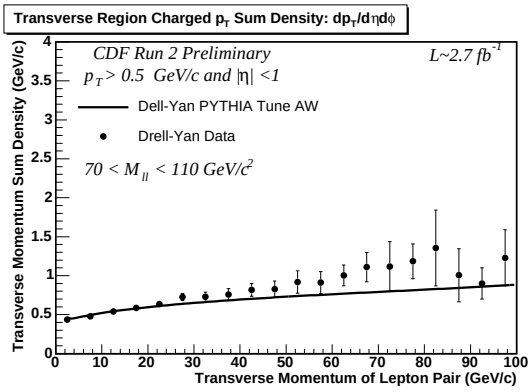

Figure 16: Transverse Region Charged P_T Sum Density, Data Corrected, Electron and Muon Data Combined ($P_T > 0.5$ GeV/c and $|\eta| < 1$). Solid line represents PYTHIA Tune AW predictions and the data are corrected back to particle level (with errors that include both the statistical error and the systematic uncertainty).

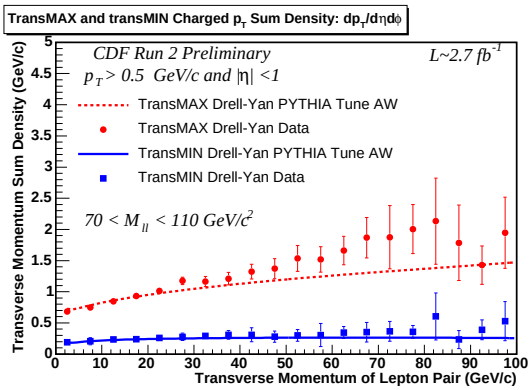

Figure 17: TransMAX and MIN Region Charged P_T Sum Density, Data Corrected, Electron and Muon Data Combined ($P_T > 0.5$ GeV/c and $|\eta| < 1$). Lines represent PYTHIA Tune AW predictions and the data are corrected back to particle level (with errors that include both the statistical error and the systematic uncertainty).

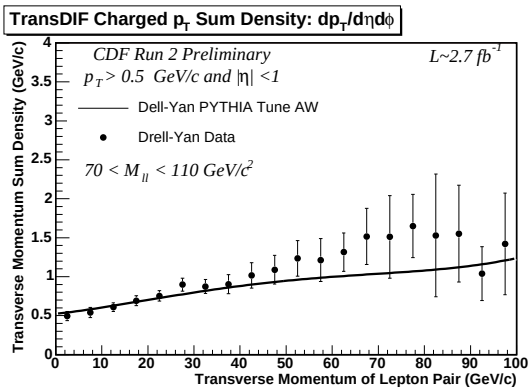

Figure 18: TransDIF Region Charged P_T Sum Density, Data Corrected, Electron and Muon Data Combined ($P_T > 0.5$ GeV/c and $|\eta| < 1$). Solid line represents PYTHIA Tune AW predictions and the data are corrected back to particle level (with errors that include both the statistical error and the systematic uncertainty).

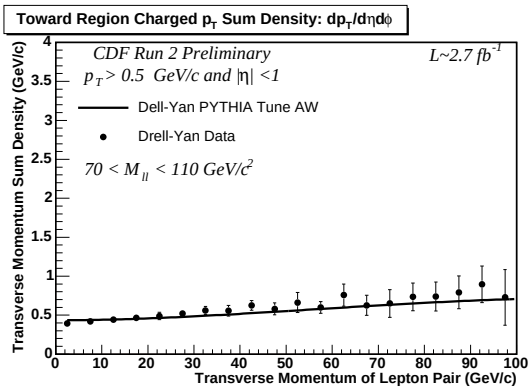

Figure 19: Toward Region Charged P_T Sum Density, Data Corrected, Electron and Muon Data Combined ($P_T > 0.5$ GeV/c and $|\eta| < 1$). Solid line represents PYTHIA Tune AW predictions and the data are corrected back to particle level (with errors that include both the statistical error and the systematic uncertainty).

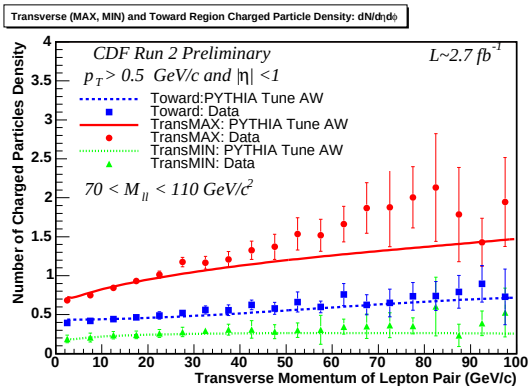

Figure 20: Transverse and Toward Region Charged P_T Sum Density, Data Corrected, Electron and Muon Data Combined ($P_T > 0.5$ GeV/c and $|\eta| < 1$). Lines represent PYTHIA Tune AW predictions and the data are corrected back to particle level (with errors that include both the statistical error and the systematic uncertainty).

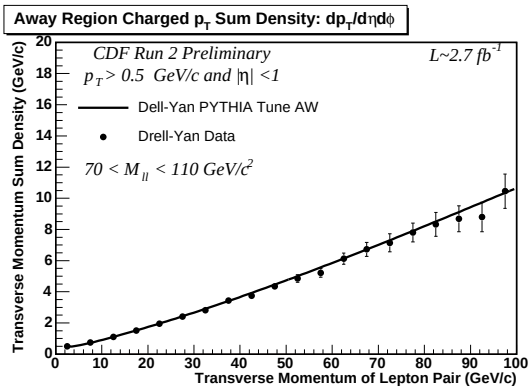

Figure 21: Away Region Charged P_T Sum Density, Data Corrected, Electron and Muon Data Combined ($P_T > 0.5$ GeV/c and $|\eta| < 1$). Solid line represents PYTHIA Tune AW predictions and the data are corrected back to particle level (with errors that include both the statistical error and the systematic uncertainty).

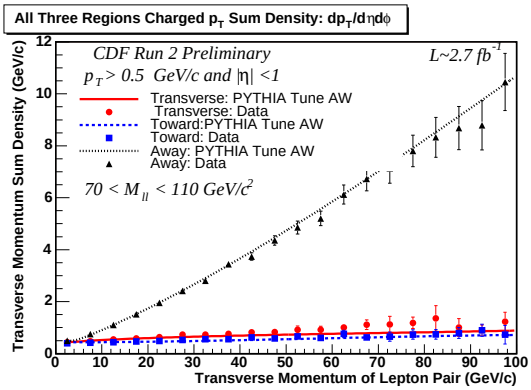

Figure 22: All Three Regions Charged P_T Sum Density, Data Corrected, Electron and Muon Data Combined ($P_T > 0.5$ GeV/c and $|\eta| < 1$). Lines represent PYTHIA Tune AW predictions and the data are corrected back to particle level (with errors that include both the statistical error and the systematic uncertainty).

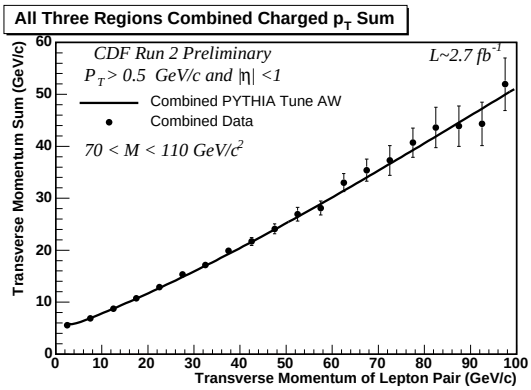

Figure 23: All Three Regions Charged P_T Sum Density Added, Data Corrected, Electron and Muon Data Combined ($P_T > 0.5$ GeV/c and $|\eta| < 1$). Solid line represents PYTHIA Tune AW predictions and the data are corrected back to particle level (with errors that include both the statistical error and the systematic uncertainty).

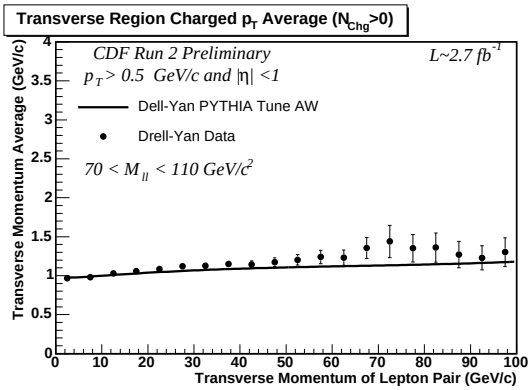

Figure 24: Transverse Region Charged P_T Average, Data Corrected, Electron and Muon Data Combined ($P_T > 0.5$ GeV/c and $|\eta| < 1$). Solid line represents PYTHIA Tune AW predictions and the data are corrected back to particle level (with errors that include both the statistical error and the systematic uncertainty).

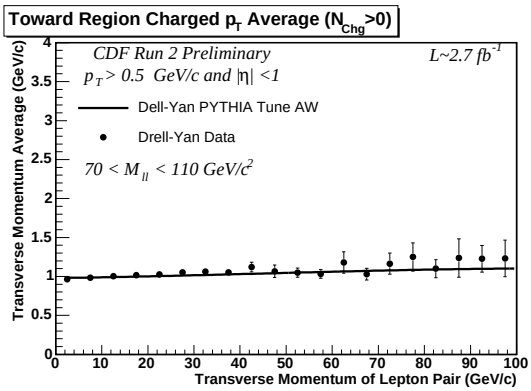

Figure 25: Toward Region Charged P_T Average, Data Corrected, Electron and Muon Data Combined ($P_T > 0.5$ GeV/c and $|\eta| < 1$). Solid line represents PYTHIA Tune AW predictions and the data are corrected back to particle level (with errors that include both the statistical error and the systematic uncertainty).

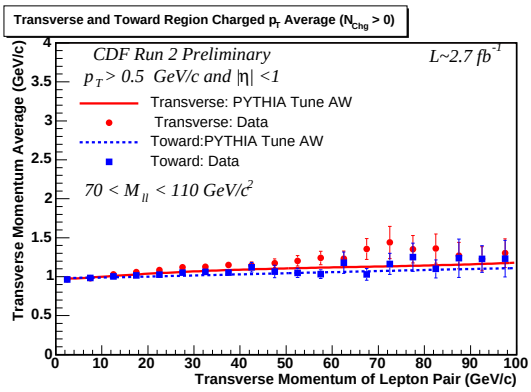

Figure 26: Transverse and Toward Region Charged P_T Average, Data Corrected, Electron and Muon Data Combined ($P_T > 0.5$ GeV/c and $|\eta| < 1$). Lines represent PYTHIA Tune AW predictions and the data are corrected back to particle level (with errors that include both the statistical error and the systematic uncertainty).

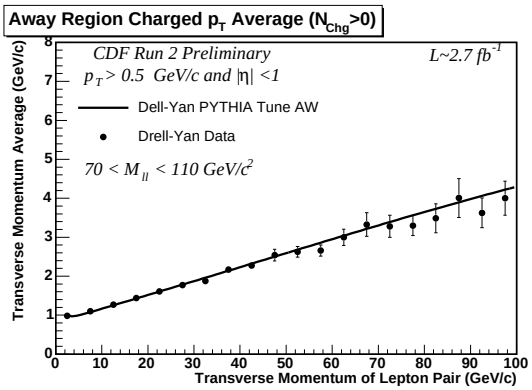

Figure 27: Away Region Charged P_T Average, Data Corrected, Electron and Muon Data Combined ($P_T > 0.5$ GeV/c and $|\eta| < 1$). Solid line represents PYTHIA Tune AW predictions and the data are corrected back to particle level (with errors that include both the statistical error and the systematic uncertainty).

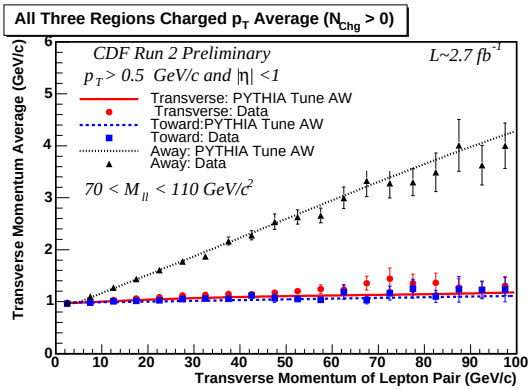

Figure 28: All Three Regions Charged P_T Average, Data Corrected, Electron and Muon Data Combined ($P_T > 0.5$ GeV/c and $|\eta| < 1$). Lines represent PYTHIA Tune AW predictions and the data are corrected back to particle level (with errors that include both the statistical error and the systematic uncertainty).

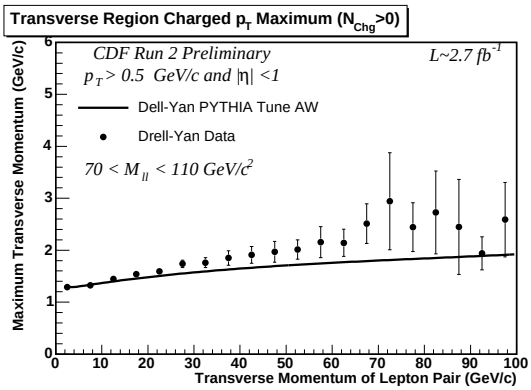

Figure 29: Transverse Region Charged P_T Maximum, Data Corrected, Electron and Muon Data Combined ($P_T > 0.5$ GeV/c and $|\eta| < 1$). Solid line represents PYTHIA Tune AW predictions and the data are corrected back to particle level (with errors that include both the statistical error and the systematic uncertainty).

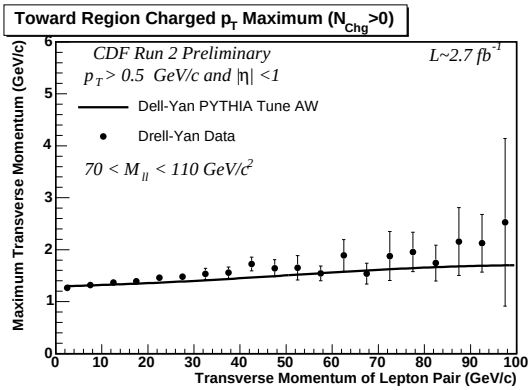

Figure 30: Toward Region Charged P_T Maximum, Data Corrected, Electron and Muon Data Combined ($P_T > 0.5$ GeV/c and $|\eta| < 1$). Solid line represents PYTHIA Tune AW predictions and the data are corrected back to particle level (with errors that include both the statistical error and the systematic uncertainty).

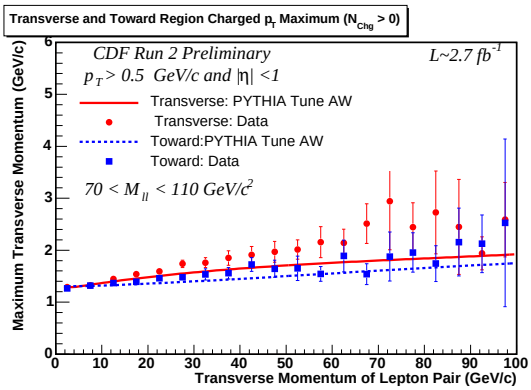

Figure 31: Transverse and Toward Region Charged P_T Maximum, Data Corrected, Electron and Muon Data Combined ($P_T > 0.5$ GeV/c and $|\eta| < 1$). Lines represent PYTHIA Tune AW predictions and the data are corrected back to particle level (with errors that include both the statistical error and the systematic uncertainty).

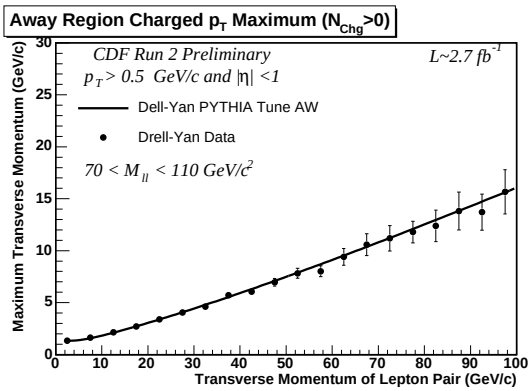

Figure 32: Away Region Charged P_T Maximum, Data Corrected, Electron and Muon Data Combined ($P_T > 0.5$ GeV/c and $|\eta| < 1$). Solid line represents PYTHIA Tune AW predictions and the data are corrected back to particle level (with errors that include both the statistical error and the systematic uncertainty).

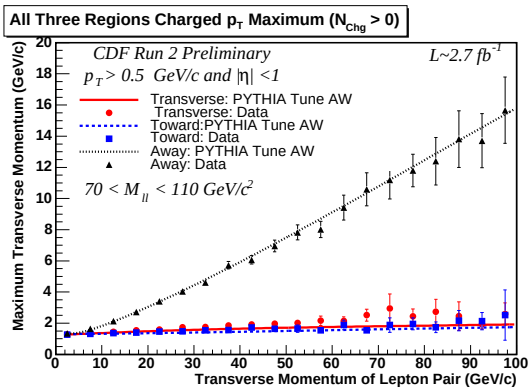

Figure 33: All Three Regions Charged P_T Maximum, Data Corrected, Electron and Muon Data Combined ($P_T > 0.5$ GeV/c and $|\eta| < 1$). Lines represent PYTHIA Tune AW predictions and the data are corrected back to particle level (with errors that include both the statistical error and the systematic uncertainty).

3.2 Comparisons with Leading Jet Underlying Event

Here we compare our results with leading jet underlying events results from [10]. Mostly we observe a very good agreement, as expected. We have to note that dijet and Drell-Yan events have distinct topologies. At very low P_T, Z-boson still has the large invariant mass, whereas we only get minbias events for dijet in that region - which explains the apparent differences between dijet and Drell-Yan 'underlying events' in low P_T region. The away-side jet in dijet events are not constrainted to be in the away region, and that explains the difference with Drell-Yan results.

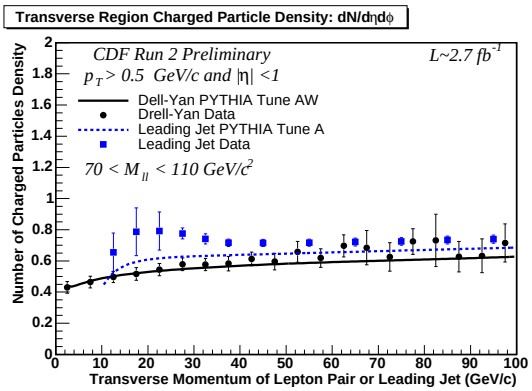

Figure 34: Transverse Region Charged Multiplicity Density, Data Corrected, Electron and Muon results combined, compared with Leading Jet result ($P_T > 0.5$ GeV/c and $|\eta| < 1$). Lines represent PYTHIA predictions and the data are corrected back to particle level (with errors that include both the statistical error and the systematic uncertainty).

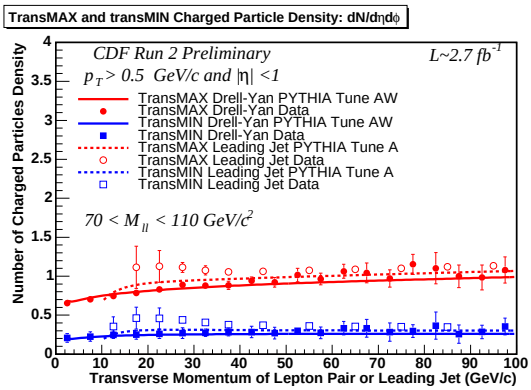

Figure 35: TransMAX and MIN Region Charged Multiplicity Density, Data Corrected, Electron and Muon results combined, compared with Leading Jet result ($P_T > 0.5$ GeV/c and $|\eta| < 1$) . Lines represent PYTHIA predictions and the data are corrected back to particle level (with errors that include both the statistical error and the systematic uncertainty).

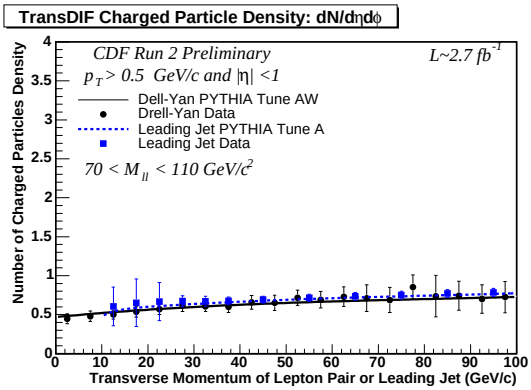

Figure 36: TransDIF Region Charged Multiplicity Density, Data Corrected, Electron and Muon results combined, compared with Leading Jet result ($P_T > 0.5$ GeV/c and $|\eta| < 1$). Lines represent PYTHIA predictions and the data are corrected back to particle level (with errors that include both the statistical error and the systematic uncertainty).

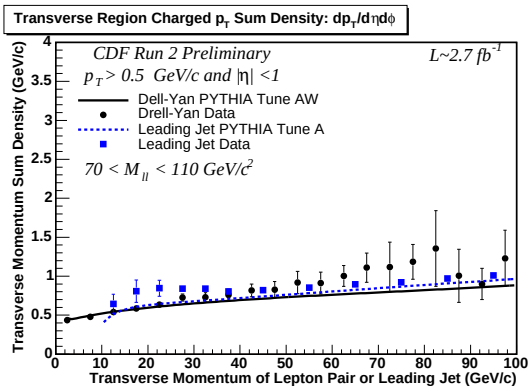

Figure 37: Transverse Region Charged P_T Sum Density, Data Corrected, Electron and Muon results combined, compared with Leading Jet result ($P_T > 0.5$ GeV/c and $|\eta| < 1$). Lines represent PYTHIA predictions and the data are corrected back to particle level (with errors that include both the statistical error and the systematic uncertainty).

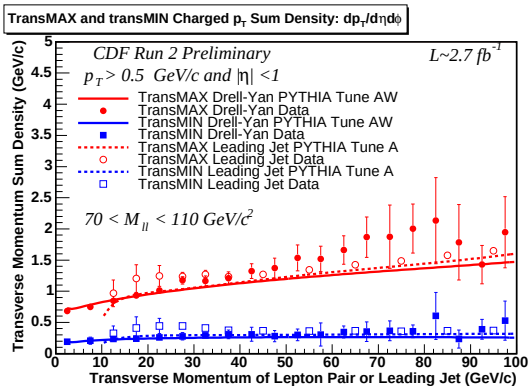

Figure 38: TransMAX and MIN Region Charged P_T Sum Density, Data Corrected, Electron and Muon results combined, compared with Leading Jet result ($P_T > 0.5$ GeV/c and $|\eta| < 1$). Lines represent PYTHIA predictions and the data are corrected back to particle level (with errors that include both the statistical error and the systematic uncertainty).

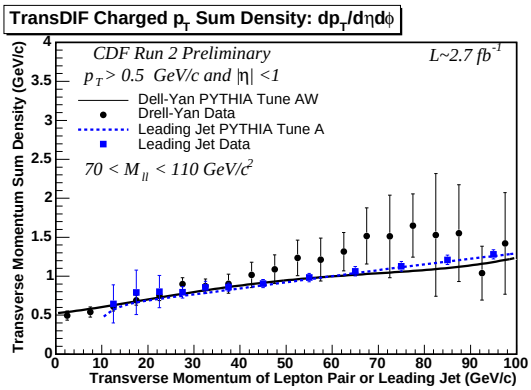

Figure 39: TransDIF Region Charged P_T Sum Density, Data Corrected, Electron and Muon results combined, compared with Leading Jet result ($P_T > 0.5$ GeV/c and $|\eta| < 1$). Lines represent PYTHIA predictions and the data are corrected back to particle level (with errors that include both the statistical error and the systematic uncertainty).

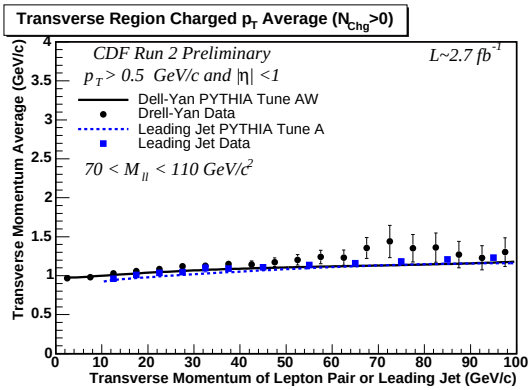

Figure 40: Transverse Region Charged P_T Average, Data Corrected, Electron and Muon results combined, compared with Leading Jet result ($P_T > 0.5$ GeV/c and $|\eta| < 1$). Lines represent PYTHIA predictions and the data are corrected back to particle level (with errors that include both the statistical error and the systematic uncertainty).

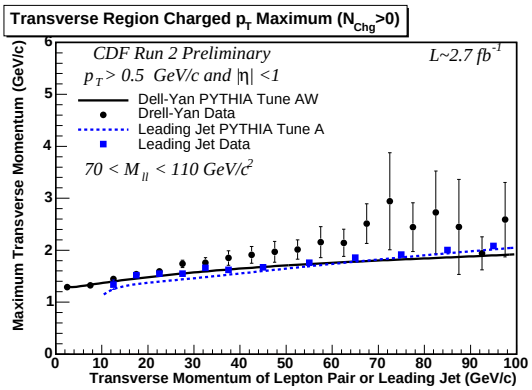

Figure 41: Transverse Region Charged P_T Maximum, Data Corrected, Electron and Muon results combined, compared with Leading Jet result ($P_T > 0.5$ GeV/c and $|\eta| < 1$). Lines represent PYTHIA predictions and the data are corrected back to particle level (with errors that include both the statistical error and the systematic uncertainty).

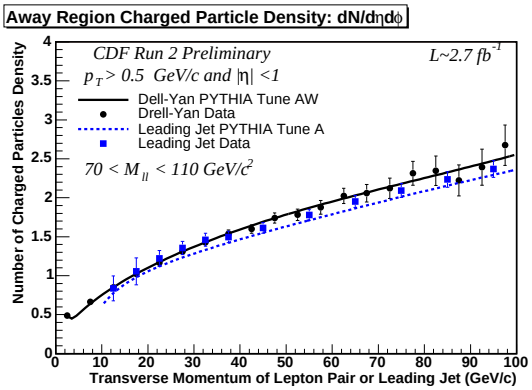

Figure 42: Away Region Charged Multiplicity Density, Data Corrected, Electron and Muon results combined, compared with Leading Jet result ($P_T > 0.5$ GeV/c and $|\eta| < 1$). Lines represent PYTHIA predictions and the data are corrected back to particle level (with errors that include both the statistical error and the systematic uncertainty).

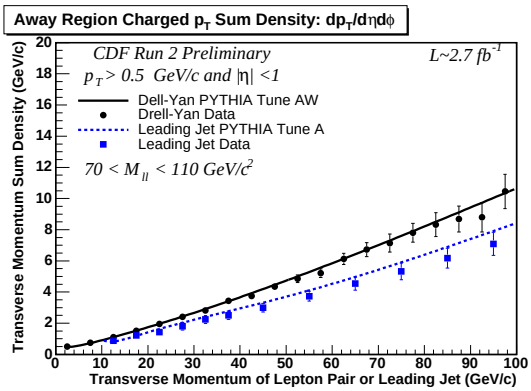

Figure 43: Away Region Charged P_T Sum Density, Data Corrected, Electron and Muon results combined, compared with Leading Jet result ($P_T > 0.5$ GeV/c and $|\eta| < 1$). Lines represent PYTHIA predictions and the data are corrected back to particle level (with errors that include both the statistical error and the systematic uncertainty).

3.3 Correlation Plots

The correlation between mean P_T and charged multiplicity is useful to look at the interplay between different mechanisms for underlying events. First we would show how the plots are arrived at, followed by the plots themselves.

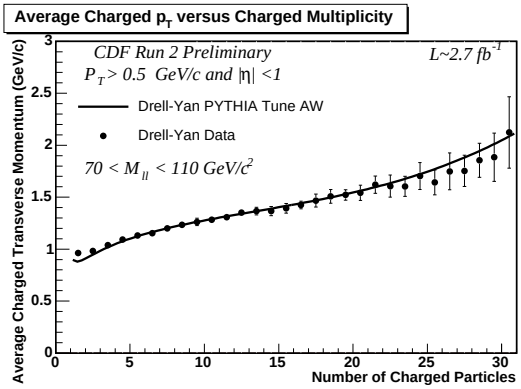

Figure 44: Drell-Yan charged p_T average and charged multiplicity correlation, electron and muon data combined ($p_T > 0.5$ GeV/c and $|\eta| < 1$). Solid line represents PYTHIA Tune AW predictions and the data are corrected back to particle level (with errors that include both the statistical error and the systematic uncertainty).

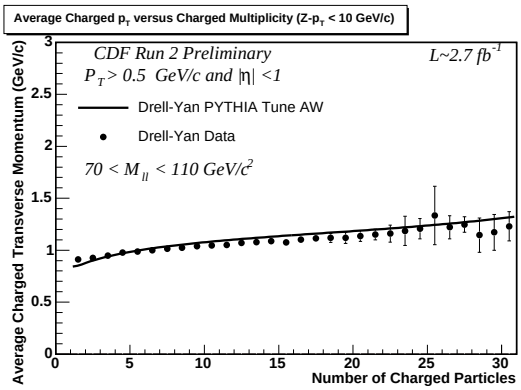

Figure 45: Drell-Yan charged p_T average and charged multiplicity correlation, with Z-p_T < 10 GeV/c, electron and muon data combined ($p_T > 0.5$ GeV/c and $|\eta| < 1$). Solid line represents PYTHIA Tune AW predictions and the data are corrected back to particle level (with errors that include both the statistical error and the systematic uncertainty).

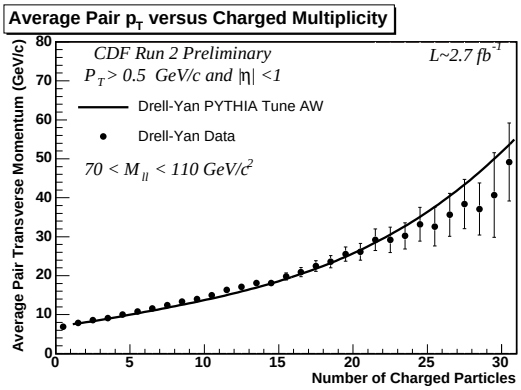

Figure 46: Drell-Yan pair p_T average and charged multiplicity correlation, electron and muon data combined ($p_T > 0.5$ GeV/c and $|\eta| < 1$). Solid line represents PYTHIA Tune AW predictions and the data are corrected back to particle level (with errors that include both the statistical error and the systematic uncertainty).

3.4 Summary

We studied the underlying event variables associated with Drell Yan lepton pair production and mostly observed excellent agreements with PYTHIA Tune AW Monte Carlo predictions. We also compared them with leading jet underlying event results and observed a reasonably close match - which may indicate the universality of underlying event modeling. For charged particle density and charged particle transverse momentum sum, we observe a slight excess at transverse region compared to toward region, which is caused by transverse regions receiving contributions from away side jet.

3.5 Summary

We studied the underlying event variables associated with Drell Yan lepton pair production and mostly observed excellent agreements with PYTHIA tune AW Monte Carlo predictions. We also compared them with leading jet underlying event results and observed reasonably close agreement - which may indicate the universality of underlying event modeling. We observe a slight excess at transverse region compared to toward region, which is caused by transverse regions receiving contributions from away side jet.

References

[1] Rick Field

Studying the Underlying Event at CDF

Proceedings 33rd International Conference on High Energy Physics (ICHEP 06), Moscow, Rssia.

[2] T. Sjostrand et al.

High-Energy-Physics Event Generation with PYTHIA 6.1

Comput. Phys. Commun. **135**, 238 (2001).

[3] Rick Field

CDF Run 2 Monte-Carlo Tunes

CDF/PHYS/JET/PUBLIC/8547.

[4] F. Abe *et al.*, The CDF Collaboration

Measurement of the Z PT Distribution in proton-Antiproton Collisions at 1.8 TeV, The CDF Collaboration

Phys. Rev. Lett. **67**, 2937-2941 (1991).

[5] A. Abulencia *et al.*, The CDF Collaboration

*Measurements of Inclusive W and Z Cross Sections in p anti-p Collisions at s**(1/2) = 1.96 TeV*

J. Phys. G: Nucl. Part. Phys. 2457-2544 (2007).

[6] D. Acosta *et al.*, CDF Collaboration

Measurement of the cross section for tt production in pp collisions using the kinematics

of lepton jets events

Physical Review D **72**, 052003 (2005).

[7] Phys. Rev. Lett. 100, 102001 (2008)

[8] G. Corcella et al.

HERWIG 6: An Event Generator for Hadron Emission Reactions with Interfering Gluons (including supersymmetric processes)

JHEP **01**, 10 (2001).

[9] J.M.Butterworth, J.R.Forshaw and M.H.Seymour

Multiparton interactions in photoproduction at HERA

Z.Phys. C**72**, 637 (1996).

[10] Alberto Cruz and Rick Field

Using Correlations in the Transverse Region to Study the Underlying Event in Run 2 at the Tevatron

CDF Public Note - CDF/PUB/JET/PUBLIC/6821

[11] Richard D.Field, Research Webpage

http://www.phys.ufl.edu/$\sim rfield/RDF\_res.html$

[12] Drell Yan figures

http://www.rarf.riken.go.jp/rarf/rhic/phys/DY/DY.html